Clinical Evaluation for System Performance of Image Intensifiers

Chang-Seon Kim, Ph.D., Charles R. Wilson, Ph.D.[¶]

Department of Radiation Oncology, Korea University Medical Center
Seoul, KOREA
[¶]Department of Radiology, Medical College of Wisconsin
Milwaukee, WI, USA

The image intensifier is the key component which determines the imaging characteristics in a fluoroscopic imaging system. A system performance program for clinical evaluation of two image intensifiers, that is simple, non-invasive and time effective, was described. Tests were grouped into three headings: x-ray generator, image quality, and collimation. For the x-ray generator, the kVp accuracy and the automatic exposure control operation were compared. Low- and high-contrast resolution measurements, and mesh pattern study belong to the image quality tests and those tests were performed for the video monitor and photospot images. For the collimation, usable field diameter and image distortion of image intensifiers were measured and quantified. The procedures and the results are hoped to be used for the clinical evaluation of system performance and/or acceptance tests for image intensifiers.

Key Words: Image intensifier, clinical evaluation, performance program, acceptance test

Introduction

A fluoroscopic imaging system consists of a x-ray tube, a generator, an image intensifier (hereafter I/I) and a patient support couch (table-top). X-ray image is converted to an optical image using an electro-optical device called an x-ray I/I. The I/I is a device that converts an incident x-ray pattern into corresponding visible light image which subsequently can be detected either on film or with a TV camera. In a well designed fluoroscopic or fluorographic imaging chain, the x-ray I/I as the front detector is the most important and the key component which provides sufficient gain to permit imaging limited by x-ray quantum statistics [1]. Any loss of image information or any noise increase occurring at this first stage is irreversible, and the characteristics of x-ray image intensifiers have, more than those of any other component, a determining effect on the final image quality. The image at the output phosphor of the I/I is coupled, via lenses, to a TV camera, where it is converted to an electrical signal for display on the monitor. An I/I may usually be operated in different magnification modes. A spot film device may be present which allows radiographic exposures to be made on a cassette [2, 3, 4, 5].

Many performance tests [1, 6-15] have been suggested for evaluating the output images from

Reprint requests to:
Chang-Seon Kim, Ph.D.
Department of Radiation Oncology
Korea University Medical Center
Seoul 136-705, KOREA
(phone) 02-920-5516, (FAX) 02-927-1419
(E-mail) ckim@nownuri.net

x-ray image-intensifying tubes. These include measurement of conversion efficiency [16], veiling glare [1, 16], high contrast resolution [16, 17], low contrast resolution [16, 17], and modulation transfer function [9, 12, 18, 19]. The quality of the output image is determined by its brightness, contrast, resolution, and the uniformity of these measurements across the screen [1, 13, 19, 20], as well as by the amount of geometric distortion in the image [6, 16, 22].

In this study, a system performance program for clinical evaluation of I/Is, that is simple, non-invasive and time effective, is presented. Tests are grouped into three headings: x-ray generator, image quality, and collimation. For the x-ray generator, the kVp accuracy and the automatic exposure control (AEC) operation are compared [16, 23]. Low-contrast and high-contrast resolution studies, and mesh pattern study belong to the image quality tests. For the collimation, actual (usable) field diameter of the I/I is measured and the image distortion is examined. While most of the tests described here are well known, it is our hope that this study will be useful for performing and documenting the clinical evaluation and/or acceptance tests of I/Is.

Methods and Materials

Two different I/Is, HX and HP/270 (General Electric Medical System, Milwaukee, USA), were installed for clinical evaluation before the routine clinical use in the Radiology Department of our hospital. All measurements were made on a GE ADVANTX in which the kVp was selectable.

Automatic Exposure Control

Automatic exposure control (AEC) of the systems was evaluated with a patient-simulating phantom. A phantom of acrylic 9″ × 9″ in cross section with a thickness variable from 0 to 8 inches in 2-inches increments, and with a lead plate 9″ × 9″ × 3/16″ thick was used. The phantom with different thickness was positioned on the table-top and between the x-ray source and I/I to approximate normal clinical geometry (nominal source-to-I/I distance of 30 inches) and was observed if the brightness on the image is maintained.

Medium fluoro detail mode was used and the grid was in the field. The I/I was positioned in the highest position. Exposure meter (MDH Ionization Monitor with 10X5-6 Chamber, Radical Co.) was positioned on the table-top and at the center of the each viewing area. Ion chamber exposure measuring systems with both rate and integrate modes was used to measure the phantom exit exposure with the exit exposure rate measured as close as possible to the intensifier input. For measurements, the exposure rate was that "chosen" by the automatic exposure rate for the phantom. The exposure rate (R/min or mR/min) was measured to quantify the AEC operation for two I/Is. Whole range of tube output, minimum to maximum, was tested.

kVp Accuracy

For the check of the kilovoltage (kVp), a non-invasive probe capable of use under low mA conditions is highly desirable and mA values less than 4 mA were used. The I/I was at 8 1/2 inches above the table and the grid was in the field. High Fluoro detail mode was selected in the test. The agreement between nominal kVp, 60 - 120 kVp, and measured kVp was evaluated using the RMI digital kVp meter (model 230) which was located on the table-top.

Low Contrast Resolution

Evaluation of low contrast resolution of the I/I takes place at 2 percent contrast level [11, 24].

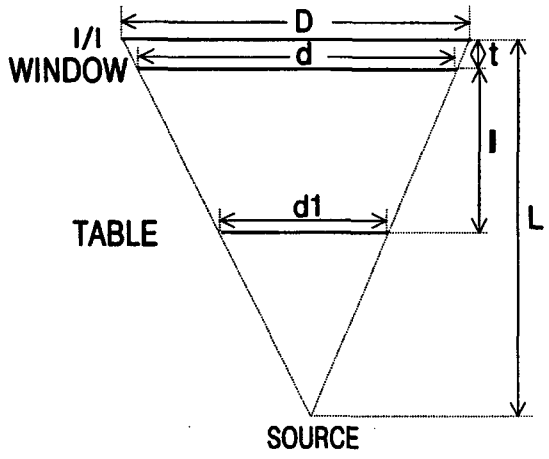

$$D = \frac{t}{I}(d - d1) + d$$

Fig. 1. Geometry and equation for determination of actual (usable) field diameter of the I/I. (Not drown to scale.) In this figure, D = The actual diameter of I/I calculated; t = The distance between the input window and the I/I; I = The distance between the input window and table-top; d = Virtual diameter of I/I in the film when the grid is located at the input window of the I/I; d1 = Virtual diameter of I/I in the film when the grid is located on table-top; L = The distance between the x-ray source and the I/I

This low contrast can be performed using a penetrometer (model 151, RMI) consisting of 1/32-inch aluminum plates. A simple tool used was an aluminum plate with holes of various sizes, diameters of 1/4, 3/16, 1/8, 1/16, and 1/32 inch, drilled in it. The low contrast phantom, two 3/4-inch thick aluminum blocks plus 1/16-inch lead plate, was positioned on the table top and the I/I was located at 8 1/2 inches above the table top. The beam size was restricted to the size of the phantom. For different fluoro detail controls - high, medium, and low, all I/I mode diameters were evaluated. In this test, grid was left in place. For these measurements, 60 kVp was employed to provide high subject contrast and the smallest visible hole size for each imaging display and/or recording mode was determined.

For low contrast resolution test on the photospot images, low contrast phantom was imaged at 80 kVp for each field size, 12, 9, 6, and 4 1/2 inches. The smallest hole diameter seen on photospot film were also determined.

High Contrast Resolution

The grid was removed to prevent mairé pattern interference between the lines of the grid and the line pattern. Focal spot size selection was 0.6 mm and the fluoro detail control was fixed, high. No absorber was in the beam and the Nuclear Associate's wedge pattern which provide resolutions ranging from 1.5 to 20 lp/mm was evaluated in the center and at the periphery of each intensifier operated in each of its four modes, 12, 9, 6, and 4 1/2 inches. The pattern was located on the input window of the I/I. The I/I was at the lowest position. Limiting resolution was determined by counting the line pairs which can be seen as viewed on the monitor. Wedge pattern was imaged using the AEC mode. Limiting resolution also judged from the photospot films.

Mesh Pattern Study

Photospots of copper screen (model 141, RMI) ranging from 16 per inch to 50 per inch were obtained in the same geometry for all four field sizes with and without the grid in the beam. Copper mesh patterns were positioned on the input window of the I/I. The I/I was positioned at 8 1/2 inches away from the table top. Tube voltage/current for the grid in and the grid out case were 120 kVp/125 mA and 80 kVp/125 mA, respectively. The fluoro detail control was fixed, high.

Measurement of Actual (Usable) Field Diameter of the Image Intensifiers

Simple geometric considerations were used to

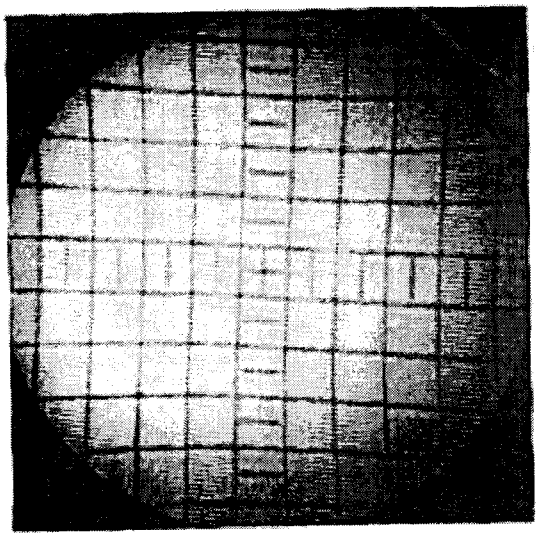

Fig. 2. A typical fluoroscopic image. S-distortion is seen along the x and y directions at the center and the pin-cushion can be seen easily at the periphery.

determine the diameter of the field of view of the image intensifier. See Fig. 1 for geometry and equation. The actual diameter can be expressed in terms of the virtual diameters of the image intensifier determined using image of a known mesh pattern placed on the table and at the input window of the image intensifier. The distances to I/I from the table and from the input window were measured. The I/I was at the lowest position. A copper grid (8 per inch) placed on the table and at the input window were imaged to use the proportionality in the geometrical structures. Two different mesh patterns were use.

Image Distortion

Geometric distortion may have three causes; an inherent effect due to the curvature of the I/I input screen, an effect dependent on the aperture of the optical coupling, and a possible contribution from TV scan non-linearities [2, 12]. A further cause of distortion is the ambient magnetic field which introduces S-distortion by its effect on the electron paths within the intensifiers. Fig. 2 shows a typical fluoroscopic image. Pin-cushion and S-distortion are mixed.

Image of a plastic matrix provides a check on geometric distortion and a measurement of the field sizes in various modes of operation. The plastic grid (8 per 10 cm) was placed at the input window of image intensifier and photospot images were taken for all field of views. The kVp was adjusted to 60 kVp and the system was operated in the AEC mode. A photospot image of the grid pattern was recorded and the degree of distortion was determined. The distortion was determined in the positive x and positive (or negative) y directions. Percent deviation from the expected position of the grid line and also the variation, and absolute deviation, as a function of distance from the center, were determined.

Results and Discussions

Automatic Exposure Control

The results of the test are given in the Table 1. Exposure rates were measured as a function of a number of variables including kVp, mA, phantom thickness, and I/I mode. The maximum table-top exposure rates are the same for systems HX and HP/270. When I/I modes are switched into smaller diameter, the exposure rate on the beam exit side of the phantom is expected to increase as the approximate ratio of the areas of the visual intensifier field in each imaging mode. The AEC mode were functioned well for the 8" thick acrylic plus 3/16" lead combined phantom for the HX and HP/270 I/Is.

kVp Accuracy

Table 2 shows the result of the kVp accuracy measurements for GE ADVENTX using HX and HP/270 I/Is. The kVp meter sensitivity is such that it typically did not respond until kVp of 85 for HX and higher for HP/270 was achieved

Table 1. Effect of plate thickness versus Image Intensifier Diameter; (a) HX, (b) HP/270

(a)

Acrylic Phantom Thickness	Modes							
	12″		9″		6″		4 1/2″	
	kVp/mA	Exp Rt.[T]	kVp/mA	Exp Rt.	kVp/mA	Exp Rt.	kVp/mA	Exp Rt.
0″	60 / 0.1	85	60 / 0.1	125	60 / 0.2	225	60 / 0.3	400
2″	60 / 0.3	350	60 / 0.4	497	60 / 0.7	872	60 / 1.4	1.57
4″	60 / 0.9	1.26	60 / 1.4	1.83	60 / 2.9	3.35	65 / 4.0	4.7
6″	60 / 3.2	4.35	61 / 4.6	60	79 / 2.7	5.2	108 / 1.7	5.4
8″	75 / 2.9	6.1	91 / 2.1	5.9	120 / 1.7	6.4	120 / 1.7	6.0
+ 3/16″ lead	120 / 1.7	7.6	120 / 1.7	7.1	120 / 1.7	6.5	120 / 1.7	6.1

(b)

Acrylic Phantom Thickness	Modes							
	12″		9″		6″		4 1/2″	
	kVp/mA	Exp Rt.	kVp/mA	Exp Rt.	kVp/mA	Exp Rt.	kVp/mA	Exp Rt.
0″	60 / 0.1	100	60 / 0.1	150	60 / 0.2	266	60 / 0.4	467
2″	60 / 0.3	430	60 / 0.4	615	60 / 0.9	1.07	60 / 1.7	1.90
4″	60 / 1.1	1.46	60 / 1.7	2.24	60 / 3.3	3.89	65 / 3.4	4.8
6″	60 / 4.0	5.32	71 / 3.0	5.15	79 / 2.3	5.13	108 / 1.6	5.55
8″	83 / 2.3	5.80	101 / 1.6	6.0	120 / 1.6	6.3	120 / 1.6	5.9
+ 3/16″ lead	120 / 1.6	7.5	120 / 1.6	7.0	120 / 1.6	6.4	120 / 1.6	5.95

[T] Exp Rt (Exposure rate) in mR/min or R/min

Table 2. kVp Accuracy Measurement for GE ADVENTX Using HX and HP/270 Image Intensifiers.

kVp setting	12″		9″		6″		4 1/2″	
	mA	kVp[T]	mA	kVp	mA	kVp	mA	kVp
60	3.9 / 2.5[¶]	No / No[†]	3.9 / 2.5	No / No	3.9 / 2.5	No / No	3.9 / 2.5	No / No
70	2.8 / 1.7	No / No	2.8 / 1.7	No / No	2.8 / 1.7	No / No	2.8 / 1.9	No / No
80	2.2 / 1.3	No / No	2.2 / 1.3	No / No	2.2 / 1.3	No / No	2.2 / 1.3	No / No
85	2.2 / 1.2	86.8 / No	2.0 / 1.2	87.5 / No	2.0 / 1.2	87.7 / No	2.0 / 1.2	87.6 / No
90	1.8 / 1.1	91.4 / No	1.8 / 1.1	91.4 / No	1.8 / 1.1	91.4 / No	1.8 / 1.1	91.6 / No
100	1.5 / 0.9	100.3 / 101.6	1.5 / 0.9	100.3 / 101.7	1.5 / 0.9	100.3 / 101.7	1.5 / 0.9	100.8 / 101.9
110	1.4 / 0.8	109.4 / 110.6	1.4 / 0.8	109.4 / 110.7	1.4 / 0.8	109.7 / 110.8	1.4 / 0.8	109.8 / 111.1
120	1.3 / 0.7	118.9 / 118.9	1.3 / 0.7	118.9 / 118.5	1.3 / 0.7	118.9 / 119.3	1.3 / 0.7	118.9 / 119.1

[T] kVp measured

[†] No kVp reading using kVp meterl

[¶] Results for HX / HP

by the unit. For both two I/Is, there was good agreement (< 3 % difference) between the set and observed kVp on both units.

Low Contrast Resolution

The displayed and recorded images are viewed and the smallest hole of the 2 % contrast penetrometer visible in the image is noted (Table

Table 3. Results of Low Contrast Resolution Measurement Using HX and HP/270 Image Intensifiers; (a) Video Monitor, (b) Photospot Images. (Upper and lower low for each cell denotes HX and HP/270, respectively.)

(a)

Fluoro Detail	12″		9″		6″		4 1/2″	
	# hole	kVp/mA	# hole	kVp/mA	# hole	kVp/mA	# hole	kVp/mA
High	4	66 / 4.0	4	71 / 3.3	4	81 / 2.7	5	100 / 1.9
	4	65 / 4.1	4	72 / 3.3	4	83 / 2.5	4	101 / 1.9
Medium	3	60 / 3.9	4	62 / 4.6	4	70 / 3.4	4	80 / 2.8
	3+	60 / 3.6	4	70 / 3.4	4	70 / 3.4	4	83 / 2.5
Low	3	60 / 1.7	3	60 / 3.0	4	61 / 4.7	4	73 / 3.1
	3	60 / 1.5	3	60 / 3.8	4	62 / 4.5	4+	70 / 3.4

(b)

	FOV Setting			
	12″	9″	6″	4 1/2″
No. of hole that can be seen	4	4	4+	4+
	4	4	4	4

3). Low contrast resolution performance of all three systems evaluated using the monitor were equivalent. The smallest hole diameter seen on photospot film are also given in the tables. Again all systems seemed to perform similarly, however, photospot images using the HP/270 did not appear as pleasing as the HX. This was probably due to the window and level used for filming. Generally, both I/Is could achieve low contrast perceptibility of 1/8-inch hole.

Table 4. High contrast resolution measurement at the center and at the periphery. A wedge pattern whose resolution ranged 1.5 to 20 lp/mm was used. (Upper and lower low for each cell denotes HX and HP/270, respectively.)

Center				
Diameter	12″	9″	6″	4 1/2″
Video Monitor (lp/mm)	No†	No	1.75	2.2 - 2.3
	No	No	1.7	2.2
Photospot (lp/mm)	No	1.7	2.3	2.9 - 3.0
	1.7	2.0	2.8	3.1
Off Center				
Video Monitor (lp/mm)	No	No	1.8	2.0
	No	No	1.7	2.2
Photospot (lp/mm)	No	No	2.5	2.5
	No	No	1.5	2.0

†Limiting resolution is less than 1.5 lp/mm.

The spatial resolution as a function of input contrast is a straightforward measurement to obtain, and requires no dismentling of equipment for testing purposes. If changes are noted, however, direct access to the image intensifier output phosphor is required to ascertain the component of the imaging system that has changed. It should be noted, however, that this measurement is not a sensitive indicator of image quality. With direct access to the intensifier output phosphor, and the availability of a light meter, conversion factor and veiling glare measurements provide direct and more sensitive measures of I/I performance and are thus better indicators. Obtaining these measurements at least semi-annually would make it possible to follow and evaluate changes in fluoroscopic image quality to determine whether TV or intensifier maintenance or tube replacement is indicated.

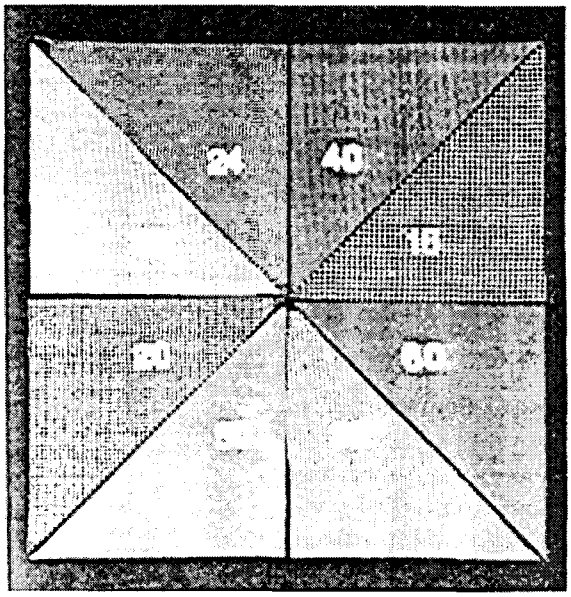

Fig. 3. Wire-mesh phantom image.

High Contrast Resolution

The Nuclear Associate's wedge pattern was evaluated in the center and at the periphery of each intensifier operated in each of its 4 modes (Table 4). Limiting resolution as viewed on the monitor in the center of the screen was less than 1.5 lp/mm for both systems operated in the 12" and 9" modes. Limiting resolution at the periphery of the image intensifiers followed a similar pattern as seen in the center of the image intensifiers. There was a slight loss of resolution compared to the center for the HX. The HP/270 shows equal limiting resolutions in the center and at the periphery.

Limiting resolution judged from the photospot films are also given in the table. Limiting resolution at the center of the image intensifiers seen to be slightly better with the HP/270 than the HX. Limiting resolution at the periphery of the image intensifiers, however, was lower than the center in both cases except for the HX in the 6" mode. The loss in resolution between the center and periphery was much greater than that seen on the video monitor.

Mesh Pattern Study

Fig. 3 is one of images of the wire-mesh phantom. For 16 per inch mesh pattern, both systems performed in a similar fashion. The HP/270 system, however, seemed to have greater distortion when compared to the HX operated in the 12" mode. Other mesh patterns were imaged equivalently. Nothing remarkable about any of the images except that the expected resolution at the periphery of the image intensifier is not as good as at the center. There is very little difference, however, between two I/Is. Resolution in the center was significantly better with the HX system than the version of the HP. For 30, 40, and 50 per inch mesh patterns, all the images have aliasing with the grid in the beam.

Measurement of Actual (Usable) Field Diameter of the Image Intensifiers

There was good agreement between the geometrically measured diameter and the nominal diameter for all image intensifiers at the 6 and 4 1/2" modes of operation. The HX and HP systems both were approximately 3/4" smaller than the nominal 9" diameter. In the 12" mode, the HX and HP/270 were approximately 1 1/2" smaller than the nominal 12" diameter. Two different mesh patterns were in good agreement as seen in the Table 5.

Table 5. Measurement of actual (usable) field diameter of I/I. (Upper and lower low in each cell denotes two results using a plastic mesh and plane scales, respectively.)

FOV setting	12"	9"	6"	4 1/2"
HX				
Actual diameter	10.28	8.15	6.03	4.45
of I/I calculated	10.78	8.27	6.24	4.52
HP/270				
Actual diameter	10.39	8.27	6.10	4.54
of I/I calculated	10.35	8.16	6.08	4.56

Table 6. Test of Image Distortion: (a) 12", (b) 9", (c) 6", and (d) 4 1/2". The image distortions are expressed in terms of absolute deviation (cm) from the assumed position and percent deviation.

(a)

HX				HP/270			
Position Measured, cm		Absolute deviation, cm (Percent deviation, %)		Position Measured, cm		Absolute deviation, cm (Percent deviation, %)	
x-axis	y-axis	x-axis	y-axis	x-axis	y-axis	x-axis	y-axis
0.51	0.40	0 (0)	0 (0)	0.55	0.75	0 (0)	0 (0)
1.32	1.23	0 (0)	0 (0)	1.40	1.60	0 (0)	0 (0)
2.13	2.06	0.07 (1.41)	0 (0)	2.25	2.45	0 (0)	0 (0)
2.94	2.89	0.13 (2.04)	0.03 (0.35)	3.10	3.30	0.17 (2.58)	0.11 (1.52)
3.75	3.72	0.36 (4.53)	0.07 (0.81)	3.95	4.15	0.40 (4.81)	0.22 (2.41)
4.56	4.55	0.70 (7.24)	0.17 (1.76)	4.80	5.00	0.70 (6.88)	0.48 (4.60)
5.37	5.38	1.08 (9.50)	0.36 (3.16)	5.65	5.85	1.23 (10.09)	0.78 (6.32)
---*	6.21	---	0.61 (4.67)	---	---	---	---

(b)

HX				HP/270			
Position Measured, cm		Absolute deviation, cm (Percent deviation, %)		Position Measured, cm		Absolute deviation, cm (Percent deviation, %)	
x-axis	y-axis	x-axis	y-axis	x-axis	y-axis	x-axis	y-axis
0.87	0.42	0 (0)	0 (0)	0.75	0.98	0 (0)	0 (0)
1.92	1.52	0.18 (5.73)	0 (0)	1.85	2.08	0.08 (2.70)	0.03 (0.96)
2.97	2.62	0.18 (3.70)	0 (0)	2.95	3.18	0.16 (3.39)	0.08 (1.57)
4.02	3.72	0.33 (5.22)	0 (0)	4.05	4.28	0.31 (4.94)	0.19 (2.80)
5.07	4.82	0.55 (6.90)	0.05 (0.62)	5.15	5.38	0.55 (6.80)	0.35 (4.09)
6.12	5.92	0.84 (8.66)	0.13 (1.35)	6.25	6.48	0.88 (8.80)	0.51 (4.94)

(c)

HX				HP/270			
Position Measured, cm		Absolute deviation, cm (Percent deviation, %)		Position Measured, cm		Absolute deviation, cm (Percent deviation, %)	
x-axis	y-axis	x-axis	y-axis	x-axis	y-axis	x-axis	y-axis
1.46	0.54	0 (0)	0 (0)	1.13	0.15	0 (0)	0 (0)
2.92	2.05	0.04 (1.03)	0 (0)	2.66	1.70	0.04 (1.50)	0 (0)
4.38	3.56	0.13 (2.74)	0 (0)	4.19	3.25	0.12 (2.63)	0.06 (1.54)
5.84	5.07	0.29 (4.79)	0.02 (0.39)	5.72	4.80	0.28 (4.55)	0.10 (2.08)
---*	6.58	---	0.02 (0.30)	---	6.35	---	0.16 (2.36)

(d)

HX				HP/270			
Position Measured, cm		Absolute deviation, cm (Percent deviation, %)		Position Measured, cm		Absolute deviation, cm (Percent deviation, %)	
x-axis	y-axis	x-axis	y-axis	x-axis	y-axis	x-axis	y-axis
1.46	0.54	0 (0)	0 (0)	1.13	0.15	0 (0)	0 (0)
2.92	2.05	0.04 (1.03)	0 (0)	2.66	1.70	0.04 (1.50)	0 (0)
4.38	3.56	0.13 (2.74)	0 (0)	4.19	3.25	0.12 (2.63)	0.06 (1.54)
5.84	5.07	0.29 (4.79)	0.02 (0.39)	5.72	4.80	0.28 (4.55)	0.10 (2.08)
---*	6.58	---	0.02 (0.30)	---	6.35	---	0.16 (2.36)

* Cannot be measured

Image Distortion

There were two types of image distortions: pin-cushion distortion and a detectable amount of S-distortion. Table 6(a) - (d) includes the results of the test of image distortion for both system and each mode. For the S-distortion, along the x and y directions S-shaped line distortion can be seen in the HP units, but they are unlikely to be clinically significant. The line distortion can be neglected in the HX I/I.

Generally, distortion and deviation from expected, the pin-cushion distortion, increased with increasing distance from the center with the 12" mode suffering the largest deviations. The HX system appeared to have somewhat less distortion and change in magnification than the HP/270 system. It should also be noted that distortion was different in all systems in the x and y directions.

Conclusions

The x-ray image intensifier as the front detector is the most important and the key component of the whole fluoroscopic imaging system. At which, the noise level and in turn the final image quality of the system is determined, called quantum sink. Many performance tests including measurement of conversion efficiency, veiling glare, and modulation transfer function have been suggested for use in monitoring image intensifier performance. In this study, however, a system performance program for clinical evaluation of two image intensifiers, that is simple, non-invasive and time effective, was described. Tests were grouped into x-ray generator, image quality, and collimation. For the x-ray generator, the kVp accuracy and the automatic exposure control operation were evaluated. Low- and high-contrast resolution measurements and mesh pattern study for the video monitor and photospot images belong to the image quality tests. For the collimation, actual (usable) field diameter and image distortion of image intensifiers were examined. Based on the clinical evaluation for system performance of HP and HX/270, as both are within acceptable limit in each test, those I/Is can be clinically used. The evaluation procedures are hoped to be used for the clinical evaluation of system performance and/or acceptance tests for image intensifiers.

References

1. Joel E. Gary, John Stears, Merrill Wondrow: *Quality Control of Video Components and Display Devices.* SPIE 486 Medical Imaging and Instrumentation '84: 64-71 (1984)
2. William R. Hendee, Edward L. Chaney, Raymond P. Rossi: *Radiologic Physics, Equipment and Quality Control.* Year Book Medical Publishers, Inc., Chicago (1977)
3. Paul M. De Groot: Image Intensifier Design and Specifications. In: J. Anthony Seibert, Gary T. Barnes, Robert G. Gould. eds. *Specification, Acceptance testing and Quality Control of Diagnostic X-ray Imaging Equipment,* AAPM Medical Physics Monograph No. 20, American Institute of Physics, Woodbury, NY, pp.429-460 (1994)
4. John A. Rowlands: Fluoroscopic Systems and Viewing Considerations In: J. Anthony Seibert, Gary T. Barnes, Robert G. Gould. eds. *Specification, Acceptance testing and Quality Control of Diagnostic X-ray Imaging Equipment,* AAPM Medical Physics Monograph No. 20, American Institute of Physics, Woodbury, NY, pp.483-497 (1994)
5. Joseph Fodor, III, Jack C. Malott: *The Art and Science of Medical Radiography.* The Catholic Health Association of the United States, St. Louis, MO, pp. 195-207 (1987)
6. Donna Lee, Allan M. Sourkes, Arthur F. Holloway, Martin H. Reed: Performance

evaluation of image-intensifier tubes. Radiology 138:455-459 (1981)

7. William R. Hendee, Raymond P. Rossi: Performance specifications for diagnostic X-ray equipment. Radiology 120:409-412 (1976)
8. William R. Hendee, Raymond P. Rossi: Purchasing Diagnostic X-ray Equipment and Initial Acceptance tests. In: Robert G. Waggener, James G. Kereiakes, and Robert J. Shalek. *CRC Handbook of Medical Physics* Volume II, CRC Press, Boca Raton, FL, pp. 147-157 (1982)
9. G.A. Hay, A.R. Cowen. A physical assessment of the imaging performance of a panel-type X-ray image intensifier. Br J Radiol 54:24-28 (1981)
10. Harvey M.J., Carmichael J.H.R., Fitzgerald M., et al.: *Assurance of Quality in the Diagnostic X-ray Department.* The British Institute of Radiology, London (1988)
11. AAPM Report No. 4. *Basic Quality Control in Diagnosticl Radiology.* Diagnostic Radiology Committee Task Force on Quality Assurance Protocol. American Association of Physicists in Medicine (1981)
12. Arnold R. Cowen. The Physical Evaluation of the Imaging performance of Television Fluoroscopy and Digital Fluoroscopy Systems Using the Leeds X-ray Test Objects: A UK Approach to Quality Assurance in the Diagnostic Radiology Department. In: J. Anthony Seibert, Gary T. Barnes, Robert G. Gould, eds. *Specification, Acceptance testing and Quality Control of Diagnostic X-ray Imaging Equipment,* AAPM Medical Physics Monograph No. 20, American Institute of Physics, Woodbury, NY, pp.499-568 (1994)
13. Dev P. Chakraborty: Routine Fluoroscopic Quality Control. In: J. Anthony Seibert, Gary T. Barnes, Robert G. Gould, eds. *Specification, Acceptance testing and Quality Control of Diagnostic X-ray Imaging Equipment,* AAPM Medical Physics Monograph No. 20, American Institute of Physics, Woodbury, NY, pp.569-595 (1994)
14. John A. Rowlands: Television Camera Design and Specification In: J. Anthony Seibert, Gary T. Barnes, Robert G. Gould, eds. *Specification, Acceptance testing and Quality Control of Diagnostic X-ray Imaging Equipment,* AAPM Medical Physics Monograph No. 20, American Institute of Physics, Woodbury, NY, 461-481 (1994)
15. Raymond P. Rossi: QC Program Documentation: The University of Colorado Approach. In: J. Anthony Seibert, Gary T. Barnes, Robert G. Gould, eds. *Specification, Acceptance testing and Quality Control of Diagnostic X-ray Imaging Equipment,* AAPM Medical Physics Monograph No. 20, American Institute of Physics, Woodbury, NY, pp.1075- 1111 (1994)
16. William R. Hendee, Raymond P. Rossi, Victor M. Spitzer, et. al.: Acceptance Testing. In: William R. Hendee, ed. *The Selection and Performance of Radiologic Equipment.* Williams & Wilkins, Baltimore, pp. 98-162 (1985)
17. Raymond P. Rossi, Richard L. Wesenberg, William R. Hendee: A variable aperture fluoroscopic unit for reduced patient exposure. Radiology 129:799-802 (1978)
18. McRobbie D.W., Hancock A.P., Castellano I.A.: A figure of merit for the assessment of image intensifier systems. Br. J Radiol 65:878-884 (1992)
19. Faulkner K., Louke M.: Measurement of image-intensifier veiling. In: Moores B.M., Stieve F.E., Eriskat H., Schibilla H.: *Technical and Physical parameters for Quality Assurance in Medical Diagnostic Radiology: tolerances, Limiting Values and Appropriate Measuring Methods.* British Institute of Radiology, London, pp.125-127 (1989)
20. Luhta R., Rowlands J.A.: Origins of flare in

x-ray image intensifiers. Med Phys 17:913-921 (1990)

21. Cooney P., Maher K.P., Malone J.F.: Measurement of the uniformity of X-ray image-intensifier television systems and of the system. In: Moores B.M., Stieve F.E., Eriskat H., Schibilla H.: *Technical and Physical parameters for Quality Assurance in Medical Diagnostic Radiology: tolerances, Limiting Values and Appropriate Measuring Methods.* British Institute of Radiology, London, pp.122-125 (1989)
22. Henshaw E.T.: Quality control measurements of x-ray image intensifier television chain systems. In: Moores B.M., Stieve F.E., Eriskat H., Schibilla H.: *Technical and Physical parameters for Quality Assurance in Medical Diagnostic Radiology: tolerances, Limiting Values and Appropriate Measuring Methods.* British Institute of Radiology, London, pp.120-122 (1989)
23. Raymond P. Rossi: X-ray Generator and Automatic Exposure Control Device Acceptance Testing. In: J. Anthony Seibert, Gary T. Barnes, Robert G. Gould, eds. *Specification, Acceptance testing and Quality Control of Diagnostic X-ray Imaging Equipment*, AAPM Medical Physics Monograph No. 20, American Institute of Physics, Woodbury, NY, pp.267-301 (1994)
24. AAPM Report No. 60. *Instrumentation requirements of Diagnostic Radiological Physicists.* Report of Task Group 4 Diagnostic X-ray Imaging Committee. Medical Physics Publishing (1998)

상강화기의 임상평가

고려대학교 의과대학, 안암병원, 방사선 종양학과
¶위스콘신 의과대학, 방사선과

김 창선, 찰스 윌슨¶

상강화기는 형광 영상장치에서 영상의 특성을 결정하는 주된 요소이다. 본 연구는 두가지의 상강화기를 임상에서 평가하기 위하여 간단하고 비파괴적이며 적당한 시간내에 행할 수 있는 계의 활동 프로그램을 제시하였다. 이 프로그램은 크게 세 부분 즉, X-선 발생장치, 영상의 질, 조준으로 되어 있다. X-선의 발생장치에 대하여 관전압의 정확도와 자동노출 조절기능을 비교하였다. 영상의 질을 위해서는 저대비 및 고대비 분해능 측정, 체격자 실험 등을 수행하였으며 이 실험에서는 비디오 모니터 및 순간영상을 필름화한 영상이 이용되었다. 조준에 대해서는 상강화기의 유용한 영역의 직경과 상의 찌그러짐을 측정하고 정량적인 분석을 하였다. 이 실험들의 과정 및 결과들이 상강화기의 인수검사 및 계의 활동지수를 평가하는데 이용되기를 바란다.

중심 단어: 상강화기, 임상평가, 활동 프로그램, 인수검사